Long-term facilitation of phrenic nerve activity in cats: responses and short time scale correlations of medullary neurones

K. F. Morris, A. Arata, R. Shannon and B. G. Lindsey

Department of Physiology and Biophysics, University of South Florida Medical Center, Tampa, FL 33612-4799, USA

1. Stimulation of either peripheral chemoreceptors or nucleus raphe obscurus results in long-term facilitation of phrenic motoneurone activity. The first objective of this work was to measure the concurrent responses of neurones in the nucleus raphe obscurus, the nucleus tractus solitarii, and the regions of the retrofacial nucleus, nucleus ambiguus and nucleus retroambigualis during induction of long-term facilitation. A second goal was to assess functional relationships of the chemoresponsive raphe neurones with neurones in the other monitored locations and with phrenic motoneurones.

2. Up to thirty single medullary neurones and phrenic nerve efferent activity were recorded simultaneously in fifteen anaesthetized, paralysed, vagotomized, artificially ventilated adult cats. Carotid chemoreceptors were stimulated by close arterial injection of 200 μl of CO_2-saturated saline solution. Spike trains were analysed with cycle-triggered histograms and two statistical tests for respiratory modulation. Peristimulus-time histograms and cumulative sum histograms were used to assess responses to stimulation. Cross-correlation was used to test for non-random temporal relationships between spike trains. Spike-triggered average histograms provided evidence for functional associations with phrenic motoneurones.

3. One hundred and thirteen of 348 neurones were monitored in the nucleus raphe obscurus. The firing rates of twenty-nine raphe neurones increased during stimulation; eighteen decreased. In twenty-one pairs of concurrently monitored raphe neurones, the firing rate of one increased its activity during stimulation then decreased, while the other showed an increase that began as the rate of the former declined. Eighteen chemoresponsive raphe neurones had short time scale features in their phrenic spike-triggered averages. Short time scale features were found in cross-correlograms from 184 of 1407 neurone pairs.

4. The data suggest parallel routes by which carotid chemoreceptors influence medullary raphe neurones and support the hypotheses that mid-line respiratory-related neuronal assemblies transform information from those receptors and regulate the gain of respiratory motor output.

Prolonged or repeated stimulation of carotid chemoreceptors produces a long-term facilitation of phrenic activity. This long-term facilitation persists for at least 1·5 h and may be involved in adaptation to extended hypoxia. This response is blocked or attenuated by serotonin antagonists in cats (Millhorn, Eldridge & Waldrop, 1980). Serotonin is known to have long-lasting excitatory effects on various respiratory motoneurones (Holtman, Dick & Berger, 1986; White & Fung, 1989; Monteau, Morin, Hennequin & Hilaire, 1990; Berger, Bayliss & Viana, 1992; Lindsay & Feldman, 1993) and increases the response of phrenic motoneurones to nonserotonergic excitation (Mitchell, Sloan, Jiang, Miletic, Hayashi & Lipski, 1992).

Serotonergic neurones are found in the raphe nuclei (Palkovits, Brownstern & Saavedra, 1974; Jacobs & Azmite, 1992). Raphe neurones project to the dorsal respiratory group (DRG) and ventral respiratory group (VRG) (Connelly, Ellenberger & Feldman, 1989; Smith, Morrison, Ellenberger, Otto & Feldman, 1989) and the spinal cord (Morrison & Gebber, 1984; Holtman *et al.* 1986). Stimulation of neurones in the caudal raphe complex leads to release of 5-HT in the nucleus tractus solitarii (NTS) and ventral horn of the spinal cord (Brodin *et al.* 1990). Evoked activity in the raphe nuclei has been reported in response to whole carotid sinus nerve electrical stimulation in cats (Miura & Reis, 1969). Electrical stimulation of the nucleus

raphe obscurus mimics the facilitation of phrenic activity seen following carotid body chemoreceptor stimulation (Millhorn, 1986).

The work described here was undertaken to assess the responses of neurones in the region of the nucleus raphe obscurus during carotid chemoreceptor stimulation. A second goal was to evaluate the functional connectivity within the nucleus and between raphe neurones and neurones in the VRG and NTS. These goals represented the next steps in elucidating the role of raphe neurones in this long-term respiratory memory.

A preliminary account of the results has been published (Morris, Arata, Shannon & Lindsey, 1993).

METHODS

Spike trains of neurones were recorded simultaneously in the ipsilateral NTS including the DRG, rostral VRG (the Bötzinger and pre-Bötzinger regions) and caudal VRG (region of nucleus ambiguus and retroambigualis), the contralateral VRG, and raphe obscurus of fifteen vagotomized, artificially ventilated cats. Anaesthesia was maintained with Dial–urethane (allobarbital (60·0 mg kg^{-1}, Ciba)–urethane (240 mg kg^{-1}). Cats were paralysed with a bolus of gallamine triethiodide (2·2 mg kg^{-1}) followed by constant infusion (0·4 mg kg^{-1} h^{-1}). The animals were given additional Dial–urethane if there was an increase in blood pressure or phrenic activity in response to periodic noxious stimuli (toe pinch). Animals were maintained with an intravenous drip (2·5% dextrose in 0·225% saline, minimum 20 ml h^{-1}), dexamethasone (2 mg kg^{-1} I.V., after 2 h 0·5 mg kg^{-1} h^{-1} in I.V. drip), atropine (0·5 mg kg^{-1} I.M.) and diphenhydramine (0·8 mg kg^{-1} I.V.). When necessary, sodium bicarbonate solution (8·4%) was infused to correct metabolic acidosis, and low molecular weight dextran solution was infused to maintain a mean systemic blood pressure of at least 100 mmHg. Core temperature was maintained at 38 ± 0·5 °C with a servo-controlled heating pad. A region of the right common carotid artery caudal to the sinus area, and the right external carotid and lingual arteries rostral to the sinus area were cleared. Inflatable occlusion cuffs were placed on the lingual and common carotid arteries, and a concentric catheter was inserted into the external artery to just below the level of the sinus. The outer barrel of the concentric catheter was connected to a pressure transducer, the inner used for injection of the chemoreceptor stimulus. Carotid chemoreceptors were stimulated with 200 μl of CO_2-saturated, 0·9% saline solution, injected over a period of 30 s. In order to stimulate selectively baroreceptors as a control, blood was withdrawn into the outer tubing of the carotid catheter. The occlusion cuffs on the lingual and common carotid arteries were then inflated. Pressure in the sinus area was raised to 200 mmHg by injecting the withdrawn blood. Arterial blood was used to minimize effects on the chemoreceptors. It was usually possible to elevate the pressure for 10–30 s in this way. Series of three to six chemoreceptor stimuli at 3–5 min intervals were alternated with series of baroreceptor stimuli at the same intervals.

We analysed spike trains for responses during stimuli with peristimulus-time histograms and cumulative sum histograms derived from the peristimulus-time histograms. Confidence bands at ± 3 S.D. were constructed for the cumulative sum histograms (Davey, Ellaway & Stein, 1986). Only changes in activity exceeding these confidence limits were considered significant. Firing-rate change during carotid chemoreceptor stimulation was classified as an increase (Inc), a decrease (Dec), no change (NC) or not tested (NT). Spike trains were subjected to two statistical evaluations of respiratory modulation and a measure of respiratory modulation, η^2, was calculated (Orem & Dick, 1983; Morris, Arata, Shannon & Lindsey, 1996). Single neurones with no statistically significant respiratory modulation of their firing rates were classified as not respiratory modulated (NRM). Cycle-triggered histograms were used to classify cells with a statistically significant respiratory modulation according to the phase (inspiration (I) or expiration (E)) during which they were more active. Neurones with peak firing rates in the first half of the phase and a longer period of decrementing than of augmenting activity were classified as decrementing (Decr) cells. Cells with peak firing rates in the second half of the phase were denoted as augmenting (Aug) neurones. Neurones were further classified as phasic (P) if their firing probability was essentially zero during some part of the respiratory cycle, otherwise they were classified as tonic (T). Respiratory cells that discharged in patterns not easily categorized were denoted as Others (Segers, Shannon, Saporta & Lindsey, 1987).

The C5 phrenic nerve rootlet was desheathed and cut peripherally for subsequent placement on bipolar, silver wire, hook electrodes in a pool of mineral oil. Spike-triggered average histograms of phrenic activity provided evidence for functional associations of chemoresponsive bulbar neurones with phrenic motoneurones. Cross-correlograms with binwidths of 0·5, 1·5, 2·5 and 5·5 ms were calculated for each pair of simultaneously recorded spike trains over the entire recorded protocol to detect and evaluate effective connectivity. Other binwidths were used as necessary to assess significant features. A detectability index (DI, equal to the ratio of the maximum amplitude of departure from background, to

Figure 1. Typical responses

A, firing-rate histograms of 30 simultaneously recorded neurones in the 5 brainstem domains, during 5 carotid chemoreceptor stimuli, and induction of long-term enhancement of respiratory activity over a period of 1000 s. Caudal VRG, caudal ventral respiratory group, region of nucleus ambiguus; NTS, nucleus tractus solitarii; Rostral VRG, right rostral VRG, region of retrofacial nucleus; Raphe, mid-line raphe obscurus; Contralateral VRG, left rostral VRG; ∫Phrenic, integrated (t = 200 ms) phrenic nerve efferent activity; S, stimulus; arrow, clearing catheter. *B*, schematic of electrode penetrations into the dorsal surface of the medulla. V, caudal VRG; D, NTS; R, ipsilateral (right) rostral VRG; A, raphe obscurus; X, contralateral (left) rostral VRG. *C*, graph of response of phrenic nerve efferent activity during fifth carotid chemoreceptor stimulus (see *A*). Top trace, peak integrated, phrenic (Phr) nerve relative amplitude (amp). Middle trace, inspiratory duration; bottom trace, expiratory duration. Dotted lines indicate ± 2 S.D. from mean of prestimulus control activity.

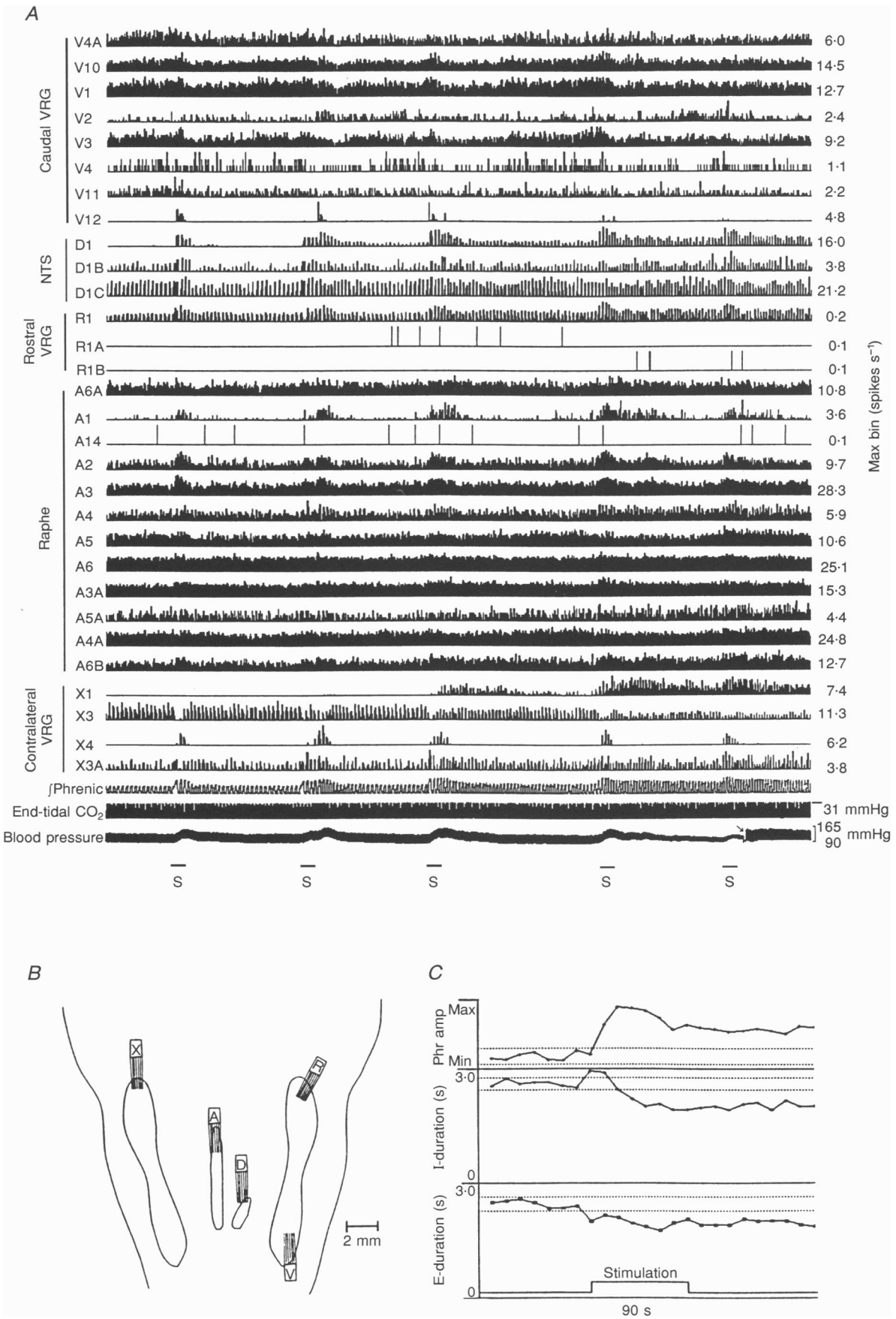

Figure 1. For legend see facing page.

Table 1. Respiratory modulation and response to carotid chemoreceptor stimulation of raphe neurones

	Response		
Resp mod	Dec	Inc	NC
E-Aug-T	3	1	3
E-Decr-T	0	5	6
E-Other	0	3	5
I-Aug-T	0	2	3
I-Decr-T	1	0	1
I-Other	2	5	5
NRM	12	13	43

Here and in subsequent tables: Resp mod, respiratory modulation; Dec, decrease; Inc, increase; NC, no change; E, expiration; Aug, augmenting; T, tonic; Decr, decrementing; I, inspiration; NRM, not respiratory modulated.

the background, divided by the S.D. of the correlogram noise) was used to test significance (Aertsen & Gerstein, 1985). Values >2 were considered significant.

At the end of the experiments, cats were given an overdose of sodium pentobarbitone and perfused with 10% neutral-buffered formalin solution. The medulla was removed and stored in the formalin solution. Brain tissue was submerged in 5% sucrose solution for at least 48 h prior to sectioning. One in three frozen sections (60 μm) was mounted, defatted, and stained with thionin. The stained sections were examined to verify the placement of electrodes. Co-ordinates of recording sites were mapped into the 3-D space of a computer-based brainstem atlas as described previously (Segers *et al.* 1987).

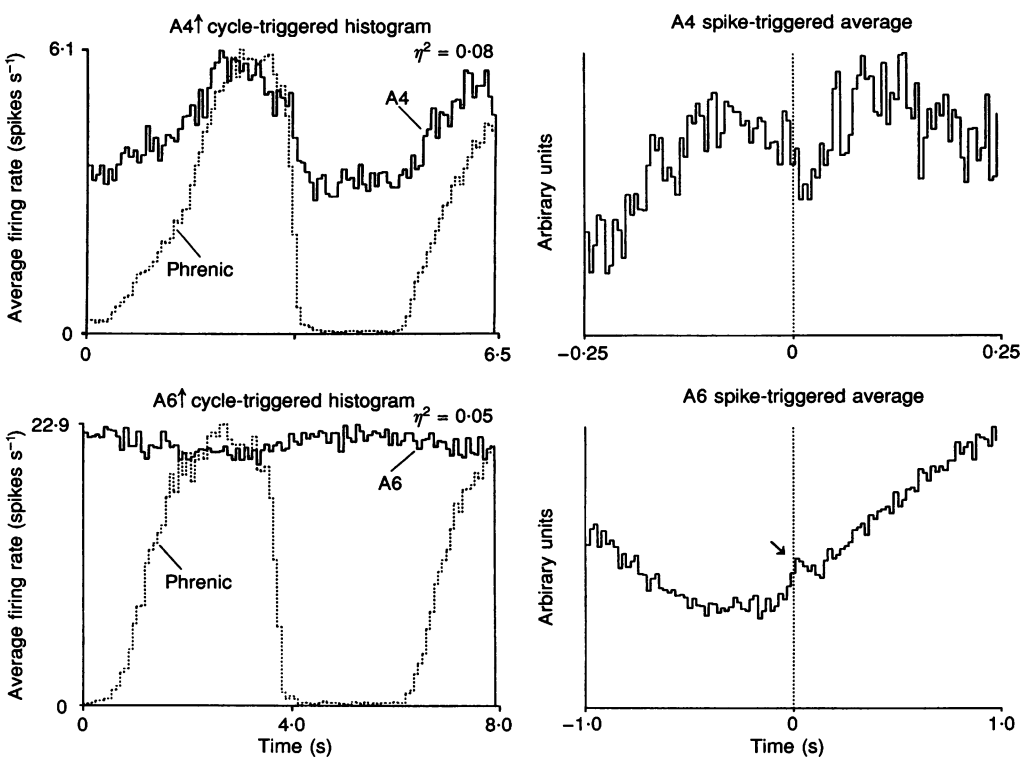

Figure 2. Two chemoresponsive respiratory modulated raphe neurones

Cycle-triggered histograms with dotted overlay of average phrenic multiunit activity help classify respiratory modulated neurones by pattern of activity; η^2 is a measurement of respiratory modulation (see Methods). Phrenic spike-triggered averages with features contribute an additional measure to help classify neurones. A4 was an I-Aug-T, responded with a significant increase in activity and showed an offset right trough in its spike-triggered average (729 cycles; 14634 spikes). A6 was an E-Other (247 cycles; 30400 spikes) neurone. The spike-triggered average at $\pm$ 1 s had an offset peak superimposed on averaged phrenic respiratory modulation relative to the activity of A6. Here and in subsequent figures, an up or down arrow after the identifier of a neurone indicates an increase or decrease, respectively, in firing rate during carotid chemoreceptor stimulation.

RESULTS

The firing rates of 113 neurones recorded in the region of the nucleus raphe obscurus during selective stimulation of carotid chemoreceptors were measured. In all experiments, neurones in other regions of the brainstem were monitored concurrently with the raphe neurones. Figure 1*A* illustrates the firing rates of thirty simultaneously monitored neurones in five brainstem domains (locations in Fig. 1*B*) during the induction of long-term facilitation of phrenic activity. Twenty-two of these neurones showed increases and decreases in firing rate during a sequence of five stimulus intervals that extended over 1000 s.

Figure 1*C* details the response of phrenic nerve activity during the fifth stimulation. There was a rapid increase in phrenic amplitude with the onset of stimulation. The first two inspiratory phases were prolonged, but subsequent inspiratory phases decreased in duration. Phrenic amplitude and frequency remained significantly increased after the stimulation ceased.

Raphe neurones were recorded from 4·5 to 1·7 mm rostral to obex, from 0·4 left to 0·6 mm right of mid-line and from 2·4 to 3·3 mm ventral to the dorsal surface of the brainstem. All 113 neurones recorded in the raphe nucleus had baseline firing rates greater than zero throughout the respiratory cycle. Forty-seven raphe neurones changed firing rate during carotid chemoreceptor stimulation; five of these changed firing rate in the same direction during the control baroreceptor stimulation. Seven raphe neurones changed firing rate in opposite directions during the two stimuli. Table 1 provides a summary of the respiratory modulation of the neurones and their responses to carotid chemoreceptor stimulation. Two examples are given in Fig. 2. The cycle-triggered histogram in each row plots the average firing rate of a single neurone as a function of time in the respiratory cycle; phrenic nerve activity is also shown (dotted line) to indicate the phases of the respiratory cycle. The up or down arrow after the identifier for each neurone in these and subsequent cycle-triggered histograms indicates an increase or decrease, respectively, in the firing rate during carotid chemoreceptor stimulation. The right histogram in each row shows the spike-triggered average of phrenic efferent activity calculated for the same neurone.

Neurone A4 was classified as I-Aug-T. It responded with an increase in activity during carotid chemoreceptor stimulation and had a trough with a positive lag in its spike-triggered average. A6 was most active during expiration. The spike-triggered average at ± 1 s shows a short time scale peak superimposed on the long time scale averaged phrenic efferent activity. The large central trough in this spike-triggered average is in agreement with the cycle-triggered histogram and indicates that A6 is more active when phrenic nerve is inactive during the expiratory phase.

Sequential increases in firing rate in pairs of simultaneously recorded raphe neurones

In twenty-one pairs of raphe neurones, the firing rate of one neurone increased during stimulation then decreased (average duration 33·6 ± 8·2 s), while the other neurone showed an increase beginning only as the former decreased (average lag from onset of stimulation 32·6 ± 8·3 s, average duration 25·5 ± 7·7 s). Figure 3 shows firing-rate histograms

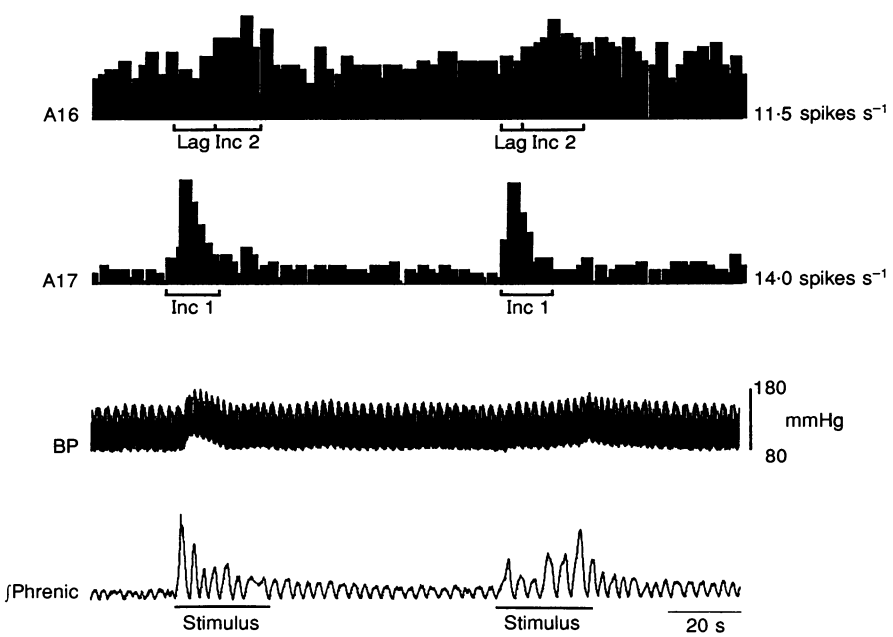

Figure 3. Firing rate histograms of two raphe neurones that alternated activity during two carotid chemoreceptor stimuli

A17 increased activity then decreased as A16 increased. BP, blood pressure.

Table 2. Numbers of cross-correlograms with significant features (S) and total simultaneously monitored pairs (To) within raphe and between raphe and the four other brainstem domains

	Raphe	cl rVRG	il rVRG	NTS	cVRG
S	65	9	30	40	40
To	232	168	305	288	414

Raphe, mid-line raphe obscurus; cl rVRG, contralateral (left) rostral ventral respiratory group; il rVRG, ipsilateral (right) rVRG; NTS, nucleus tractus solitarii; cVRG, caudal VRG.

of two simultaneously recorded raphe neurones, blood pressure, and integrated phrenic nerve activity during an interval that included two stimuli. The alternating changes in activity were not correlated with the small transient changes in blood pressure, nor with the peak of integrated phrenic response. Other concurrent responses are listed in Table 3 as described in a later section of the Results.

Raphe neurones exhibited short time scale correlations with phrenic nerve efferent fibres

Among the forty-seven raphe neurones that increased or decreased their firing rates in response to chemoreceptor stimulation, ten with respiratory modulation and five without had central features in their spike-triggered averages. One chemoresponsive, respiratory-modulated, raphe neurone had an offset peak in its spike-triggered average and two showed offset troughs. One offset trough and the offset peak were shown in Fig. 2.

Short time scale correlations of pairs of neurones

Cross-correlograms were calculated from 1407 pairs of neurones, each of which included at least one neurone recorded in nucleus raphe obscurus; 184 (13·1%) had significant features. Table 2 summarizes the fractions of neuronal pairs that exhibited short time scale correlations, by brainstem region. Numbers of pairs monitored within raphe obscurus or pairs consisting of one neurone in raphe obscurus and the second in one of the other four brainstem domains, that had significant short time scale correlations are in row 'S'. Numbers in row 'T' are total simultaneously monitored pairs.

Table 3 lists all pairs of raphe neurones with significant short time scale correlations grouped by major feature classification (central peak, central trough, offset peak, offset trough or multiple peaks and troughs). Each group is sorted alphabetically keyed first on respiratory modulation of trigger, then trigger response to carotid chemoreceptor stimulation and then target modulation and response. Measurements of significant features are given as means ± S.D. in Table 3 and in the following text and tables.

There were forty-two pairs of raphe neurones, with at least one chemoresponsive neurone, that exhibited short time scale correlations. All but three of those pairs contained at least one neurone with a respiratory modulated firing rate. The cross-correlograms of twenty-four of the forty-two pairs had central peaks as primary features (DI = 7·18 ± 3·1, HW = 27·04 ± 24·5 ms). Ten pairs had central troughs (DI = 7·99 ± 3·55, HW = 44·6 ± 29·12 ms) and seven pairs had offset peaks (DI = 4·84 ± 0·85, lag = 4·81 ± 6·98 ms, HW = 24·1 ± 23·65 ms) four of which also had offset troughs. Seventeen pairs of raphe neurones that showed central peaks or troughs as primary features in cross-correlograms also had offset troughs or peaks as significant secondary features. Figure 4 shows cross-correlograms of several pairs including two pairs of simultaneously monitored raphe neurones. A6A and A1 had a central peak with offset troughs in their cross-correlogram. Both E-Decr-T neurones increased activity during stimulation. A6A had a central peak in its phrenic spike-triggered average. A1 had no short time scale features in its spike-triggered average. The other raphe pair illustrated was E-Decr-T neurone A2 and I-Aug-T neurone A4; the firing rates of both increased activity during stimulation. Their cross-correlogram had a central trough. The offset trough in the phrenic spike-triggered average for A4 is shown in Fig. 2.

There were fifty-one significant short time scale correlations between raphe neurones and VRG neurones with at least one neurone responding to carotid chemoreceptor stimulation. These included fifteen with central peaks, four of which also had offset troughs, and five correlations with multiple peaks and troughs. Table 4 lists cross-correlograms of all pairs with significant central features that consisted of a raphe and a VRG neurone. Figure 4 shows one example. The cross-correlogram has a central peak and an offset trough with a positive lag. The I-Aug-T reference neurone V4 was recorded in the caudal VRG; its firing rate increased during carotid chemoreceptor stimulation. The firing rate of the raphe E-Aug-T target neurone A1 did not change during stimulation.

Cross-correlograms that had offset features with positive lags, from pairs of neurones composed of a VRG reference neurone and a raphe target cell, are listed in Table 5. Six pairs consisting of respiratory-modulated, chemo-

Table 3. Short time scale correlations between raphe neurones

Central peaks

Resp 1	Chemo 1	Resp 2	Chemo 2
E-Aug-T	Dec	I-Other	NC
E-Decr-T	Inc	E-Decr-T	Inc (5)
E-Decr-T	Inc	E-Other	Inc
E-Decr-T	NC	E-Decr-T	NC
E-Decr-T	NC	NRM	NC
E-Other	Inc	E-Decr-T	Inc (4)
I-Aug-T	NC	NRM	NC (2)
I-Decr-T	NC	I-Other	NC
I-Other	Inc	E-Decr-T	NC
I-Other	Inc	NRM	NC
I-Other	NC	I-Decr-T	NC
I-Other	NC	NRM	NC
NRM	Inc	E-Decr-T	Inc (3)
NRM	Inc	E-Other	Inc
NRM	Inc	NRM	Dec
NRM	Inc	NRM	Inc (3)
NRM	Inc	NRM	NC
NRM	NC	E-Decr-T	Inc
NRM	NC	E-Other	Inc
NRM	NC	NRM	NC (3)
NRM	NT	NRM	NC

Mean DI = 6·82 ± 3·38. Mean HW = 24·04 ± 23·15 ms.

Central troughs

Resp 1	Chemo 1	Resp 2	Chemo 2
E-Decr-T	Inc	I-Aug-T	Inc (3)
E-Other	Inc	I-Aug-T	Inc (2)
E-Other	NC	NRM	NC
I-Aug-T	Inc	E-Decr-T	Inc
I-Aug-T	NC	NRM	Dec
I-Decr-T	Dec	NRM	Inc
I-Other	NC	E-Decr-T	NC
I-Other	NC	I-Other	Inc
I-Other	NC	NRM	NC
NRM	Inc	I-Aug-T	Inc

Mean DI = 7·86 ± 3·13. Mean HW = 44·85 ± 28·18 ms.

Multiple peaks and troughs

Resp 1	Chemo 1	Resp 2	Chemo 2
I-Decr-T	NC	I-Decr-P	NC

Offset peaks

Resp 1	Chemo 1	Resp 2	Chemo 2
E-Aug-T	Dec	NRM	Inc
E-Decr-T	Inc	E-Decr-T	Inc
E-Decr-T	NC	I-Other	Inc
E-Decr-T	NC	NRM	NC
E-Other	Inc	E-Decr-T	Inc
E-Other	Inc	NRM	Inc
I-Decr-T	Dec	NRM	Inc
NRM	Inc	E-Decr-T	Inc
NRM	NC	NRM	NC (3)

Mean DI = 4·85 ± 1·09.
Mean lag = 8·36 ± 10·75 ms.
Mean HW = 28·41 ± 23·73 ms.

Offset troughs

Resp 1	Chemo 1	Resp 2	Chemo 2
NRM	NC	E-Aug-T	Dec
NRM	NC	E-Aug-T	NC
NRM	NC	E-Decr-T	NC
NRM	NC	NRM	NC (2)

Mean DI = 4·18 ± 1·14.
Mean lag = 24·20 ± 18·93 ms.
Mean HW = 12·10 ± 8·08 ms.

See Methods for explanation of respiratory modulation. Here and in subsequent tables: Resp 1, respiratory modulation of trigger neurone; Chemo 1, trigger neurone response to carotid chemoreceptor stimulation; Resp 2, target neurone modulation; Chemo 2, target neurone response. Primary responses to carotid chemoreceptor stimulation were classed as an increase (Inc), decrease (Dec), no change (NC) or not tested (NT). The detectability index (DI) is equal to the ratio of the maximum amplitude of departure from background, to the background, divided by the S.D. of the correlogram noise (Aertsen & Gerstein, 1985). The half-width (HW) is the duration of contiguous bins with a difference from background at least half that of the bin with the largest difference, given in milliseconds. Numbers in parentheses indicate *n*, the number of neurone pairs.

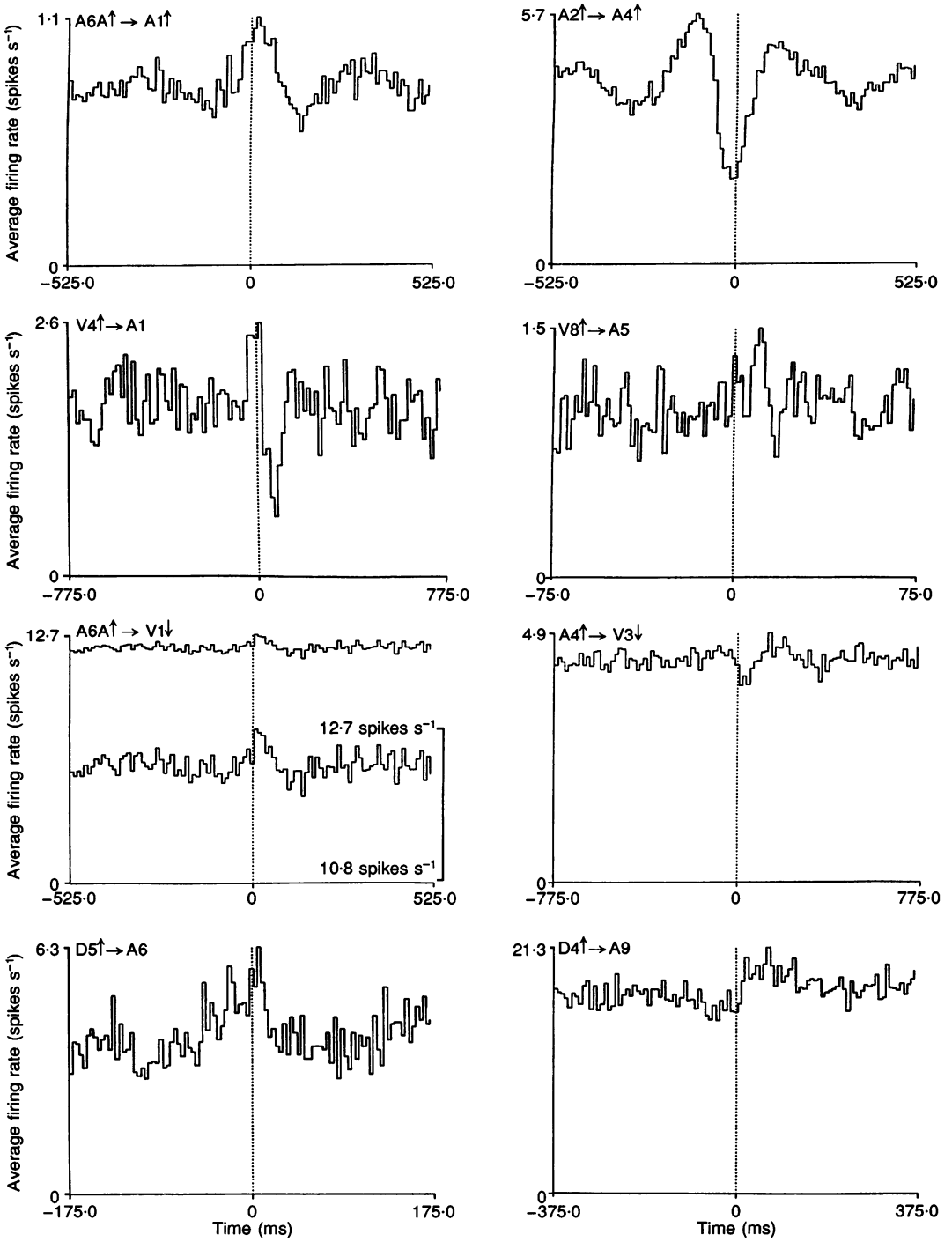

Figure 4. Correlated neurone pairs

A6A and A1 had a central peak (DI, 13·2; HW, 77·0 ms; 36 230 trigger spikes; 2388 target spikes) with offset troughs in their cross-correlogram. Both increased activity and were E-Decr-T. A6A had a central peak in its spike-triggered average but A1 showed no short time scale features. A2 and A4 had a central trough (DI, 5·5; HW, 71·5 ms; 20 057 trigger spikes; 14 669 target spikes) in their cross-correlogram. A2 and A4 were E-Decr-T and I-Aug-T, respectively, and both increased activity. In their spike-triggered averages, A2 had a central peak whilst A4 had an offset trough (see Fig. 2). The cross-correlogram of VRG neurone V4 and raphe neurone A1 shows a central peak (DI, 3·3; HW, 62·0 ms; 1994 trigger spikes; 5191 target spikes) and offset right trough (DI, 4·8; lag, 31·0 ms; HW, 46·5 ms). V4 was an I-Aug-T that increased activity during carotid chemoreceptor stimulation. A1 was an E-Aug-T that did not change rate significantly during stimulation. There was an offset right peak in the cross-correlogram for V8 trigger and A5 target (DI, 3·8; lag, 7·5 ms; HW, 6·0 ms; 32 754 trigger spikes; 3414 target spikes). V8 increased activity during carotid chemoreceptor stimulation and was an I-Aug-T whilst A5 did not change rate significantly and was not respiratory modulated. The cross-correlogram with an offset right peak (DI, 3·3;

Table 4. Short time scale correlations: raphe→VRG central features

Central peaks

Raphe→il rVRG				Raphe→cVRG				Raphe→cl rVRG			
Resp 1	Chemo 1	Resp 2	Chemo 2	Resp 1	Chemo 1	Resp 2	Chemo 2	Resp 1	Chemo 1	Resp 2	Chemo 2
E-Aug-T	Dec	E-Decr-T	NC	E-Aug-T	NC	I-Aug-P	Inc	I-Other	NC	I-Other	NC
E-Aug-T	Dec	NRM	NT	E-Decr-T	Inc	I-Aug-T	Inc	NRM	NC	NRM	NC
E-Decr-T	NC	E-Aug-P	NC	E-Decr-T	Inc	I-Other	Inc				
NRM	Dec	NRM	NC	I-Aug-T	Inc	NRM	Inc				
NRM	Inc	E-Aug-T	NC	I-Decr-T	NC	NRM	NC				
NRM	Inc	E-Decr-T	NC	I-Other	Inc	NRM	NC				
NRM	Inc	NRM	NC	I-Other	NC	I-Other	Inc				
NRM	NC	E-Decr-T	NC	NRM	Inc	I-Aug-T	Inc				
NRM	NC	I-Aug-T	NC	NRM	NC	E-Decr-T	Dec (2)				
NRM	NC	NRM	NC								
NRM	NC	NRM	NT								
Mean DI = 4·00 ± 0·64. Mean HW = 13·05 ± 12·64.				Mean DI = 3·40 ± 0·38. Mean HW = 16·90 ± 13·48.				Mean DI = 3·35 ± 0·05. Mean HW = 5·50 ± 0·00.			

Central troughs

Raphe→il rVRG				Raphe→cVRG			
Resp 1	Chemo 1	Resp 2	Chemo 2	Resp 1	Chemo 1	Resp 2	Chemo 2
NRM	NC	NRM	NC	E-Decr-T	NC	I-Other	Inc

Multiple peaks and troughs

Raphe→il rVRG				Raphe→cVRG				Raphe→cl rVRG			
Resp 1	Chemo 1	Resp 2	Chemo 2	Resp 1	Chemo 1	Resp 2	Chemo 2	Resp 1	Chemo 1	Resp 2	Chemo 2
I-Other	NC	NRM	Dec	E-Decr-T	NC	NRM	NC	E-Decr-T	NC	I-Other	NC
NRM	Inc	I-Aug-P	Inc	NRM	NC	I-Aug-T	Inc	E-Decr-T	NC	E-Aug-P	NC
NRM	NC	I-Decr-T	NC	NRM	NC	NRM	Inc	I-Other	Inc	I-Other	NC

responsive caudal VRG reference neurones and target neurones in the raphe, had offset peaks in cross-correlograms. One such offset peak was also shown in Fig. 4; I-Aug-T reference neurone V8 increased activity during carotid chemoreceptor stimulation; target neurone A5 did not change rate significantly and was not respiratory modulated.

Table 6 lists cross-correlograms that had offset primary features with positive lags when the raphe neurone of the pair and the neurone recorded in the region of the VRG were used as reference and target neurones, respectively. Offset peaks with positive lags were detected in cross-correlograms for seven pairs, each composed of a raphe neurone that responded with an increased firing rate

lag, 11·0 ms; HW, 27·5 ms; 36 230 trigger spikes; 42 910 target spikes) of A6A (also correlated with A1 (top left)) and V1 has an absolute scale on left and the same cross-correlogram superimposed and scaled up indexed on right. I-Aug-T neurone V1 (729 cycles; 42 962 spikes) increased then decreased activity. The cross-correlogram of A4 (see Fig. 2 and above) and V3 has an offset right trough (DI, 3·4; lag, 15·5 ms; HW = 46·5 ms; 14 671 trigger spikes; 14 916 target spikes). V3 was an I-Aug-T (729 cycles; 14 936 spikes) that increased then decreased activity during stimulation and had no features in its spike-triggered average. D5 in NTS and A6 in raphe were both NRM neurones. D5 increased activity during carotid chemoreceptor stimulation. Their cross-correlogram had a broad central peak (DI = 5·8; HW = 7·0 ms; 5100 trigger spikes; 14 253 target spikes). NTS neurone D4 was an NRM that increased activity during carotid chemoreceptor stimulation. Its cross-correlogram with target cell A9, an E-Decr-T that did not change firing rate, has a broad offset peak to the right (DI = 4·9; lag = 15·0 ms; HW = 82·0 ms; 3136 trigger spikes; 50 662 target spikes).

Table 5. Short time scale correlations: VRG→raphe offset features

Offset peaks

il rVRG→Raphe			
Resp 1	Chemo 1	Resp 2	Chemo 2
E-Other	NC	NRM	Inc
I-Decr-P	NC	E-Other	NC
NRM	Inc	NRM	NC
NRM	NT	NRM	Inc
NRM	NT	NRM	NC

Mean DI = 4·56 ± 1·08.
Mean lag = 21·90 ± 25·15 ms.
Mean HW = 14·60 ± 9·79 ms.

cVRG→Raphe			
Resp 1	Chemo 1	Resp 2	Chemo 2
E-Decr-T	Dec	NRM	NC
E-Other	NC	E-Aug-T	NC
I-Aug-T	Inc	NRM	Inc
I-Aug-T	NC	NRM	NC
I-Decr-P	Inc	I-Aug-T	NC (2)
I-Decr-T	Inc	NRM	Inc
I-Other	Inc	E-Aug-T	NC
NRM	Inc	NRM	NC

Mean DI = 4·12 ± 1·36.
Mean lag = 9·17 ± 9·07 ms.
Mean HW = 12·56 ± 13·60 ms.

cl rVRG→Raphe			
Resp 1	Chemo 1	Resp 2	Chemo 2
E-Aug-P	NC	I-Other	NC
I-Other	NC	E-Decr-T	NC
NRM	Inc	NRM	NC

Mean DI = 3·17 ± 0·66.
Mean lag = 17·00 ± 19·16 ms.
Mean HW = 10·17 ± 5·54 ms.

Offset troughs

il rVRG→Raphe			
Resp 1	Chemo 1	Resp 2	Chemo 2
NRM	Dec	E-Decr-T	NC

cVRG→Raphe			
Resp 1	Chemo 1	Resp 2	Chemo 2
I-Decr-P	NC	E-Aug-T	Inc
I-Other	Inc	E-Decr-T	NC
I-Other	Inc	I-Other	Inc

Mean DI = 3·63 ± 0·34.
Mean lag = 19·83 ± 10·84 ms.
Mean HW = 4·17 ± 1·89 ms.

Table 6. Short time scale correlations: raphe→VRG offset features

Offset peaks

Raphe→il r VRG			
Resp 1	Chemo 1	Resp 2	Chemo 2
E-Aug-T	NC	NRM	NT (2)
E-Decr-T	Inc	I-Decr-P	NC
NRM	NC	I-Other	Inc
NRM	NC	NRM	NC
NRM	NT	I-Aug-T	Dec

Mean DI = 4·98 ± 1·87.
Mean lag = 11·70 ± 5·82 ms.
Mean HW = 21·90 ± 22·62 ms.

Raphe→cVRG			
Resp 1	Chemo 1	Resp 2	Chemo 2
E-Decr-T	Inc	I-Aug-T	Inc (4)
E-Decr-T	Inc	I-Other	Inc
E-Decr-T	NC	NRM	NC
E-Other	Inc	I-Aug-T	Inc
I-Other	Inc	NRM	NC
NRM	Inc	I-Other	Inc
NRM	NC	E-Decr-T	NC
NRM	NT	NRM	NC

Mean DI = 3·64 ± 0·65.
Mean lag = 18·55 ± 21·27 ms.
Mean HW = 14·73 ± 12·59 ms.

Raphe→cl rVRG			
Resp 1	Chemo 1	Resp 2	Chemo 2
I-Other	Inc	E-Aug-P	NC

Offset troughs

Raphe→il rVRG			
Resp 1	Chemo 1	Resp 2	Chemo 2
NRM	NC	NRM	NT (3)

Mean DI = 6·43 ± 2·33.
Mean lag = 47·67 ± 6·86 ms.
Mean HW = 45·83 ± 25·54 ms.

Raphe→cVRG			
Resp 1	Chemo 1	Resp 2	Chemo 2
I-Aug-T	Inc	I-Aug-T	Inc
I-Aug-T	Inc	I-Other	Inc
NRM	NT	NRM	Dec

Mean DI = 2·87 ± 0·2.
Mean lag = 40·33 ± 14·73 ms.
Mean HW = 11·0 ± 5·5 ms.

Table 7. Short time scale correlations: raphe→NTS

Raphe→NTS

Central peaks

Resp 1	Chemo 1	Resp 2	Chemo 2
E-Aug-T	Dec	I-Decr-P	NC
E-Decr-T	NC	E-Decr-P	NC
I-Other	NC	I-Aug-T	NC
I-Other	NC	I-Other	Inc
I-Other	NC	NRM	NT
I-Other	NC	NRM	NC
NRM	Inc	NRM	Dec
NRM	NC	I-Aug-P	Dec
NRM	NC	NRM	NC
NRM	NC	NRM	Inc

Mean DI = 4·70 ± 1·66.
Mean HW = 13·75 ± 10·79 ms.

Central troughs

Resp 1	Chemo 1	Resp 2	Chemo 2
E-Decr-T	NC	NRM	NC
I-Other	Inc	I-Other	Inc
I-Other	Inc	NRM	NC
I-Other	Inc	NRM	Inc

Mean DI = 3·23 ± 0·37.
Mean HW = 8·25 ± 2·75 ms.

Multiple peaks and troughs

Resp 1	Chemo 1	Resp 2	Chemo 2
E-Decr-T	NC	I-Aug-T	NC (2)
E-Decr-T	NC	NRM	NC
I-Other	NC	NRM	NC
NRM	Inc	NRM	Dec
NRM	Inc	NRM	NC
NRM	NC	I-Other	Inc
NRM	NC	NRM	NC

Offset peaks

NTS→Raphe

Resp 1	Chemo 1	Resp 2	Chemo 2
E-Decr-P	NC	NRM	NC
I-Decr-P	NC	NRM	NC
I-Other	Inc	E-Decr-T	NC (2)
NRM	Inc	E-Decr-T	NC (2)
NRM	Inc	NRM	NC (2)
NRM	NC	NRM	NC

Mean DI = 4·40 ± 1·04.
Mean lag = 32·33 ± 37·01 ms.
Mean HW = 11·07 ± 5·80 ms.

Raphe→NTS

Resp 1	Chemo 1	Resp 2	Chemo 2
I-Other	NC	NRM	Inc
NRM	Dec	NRM	Inc (2)
NRM	Inc	NRM	Inc
NRM	NC	NRM	NC

Mean DI = 3·36 ± 0·40.
Mean lag = 10·90 ± 11·21 ms.
Mean HW = 9·50 ± 9·59 ms.

Offset troughs

NTS→Raphe

Resp 1	Chemo 1	Resp 2	Chemo 2
I-Aug-P	Dec	E-Decr-T	NC
NRM	NC	I-Other	Inc

Mean DI = 2·70 ± 0·40.
Mean lag = 11·00 ± 11·00 ms.
Mean HW = 5·50 ± 0·00 ms.

Raphe→NTS

Resp 1	Chemo 1	Resp 2	Chemo 2
E-Decr-T	NC	NRM	NC
I-Other	NC	E-Decr-P	NC

Mean DI = 3·50 ± 0·80.
Mean lag = 27·25 ± 16·75 ms.
Mean HW = 16·25 ± 5·75 ms.

during carotid chemoreceptor stimulation and a respiratory modulated neurone in the caudal VRG. The cross-correlogram of one pair is shown in Fig. 4. The E-Decr-T raphe neurone A6A had a central peak in its phrenic spike-triggered average. Activity in I-Aug-T neurone V1 first increased then decreased during chemoreceptor stimulation.

Offset troughs with positive lags were the primary features in cross-correlograms for two pairs, each consisting of a respiratory modulated raphe neurone that increased its activity during chemoreceptor stimulation and a respiratory modulated caudal VRG neurone. An example of this transient decline in firing probability is shown in Fig. 4. The I-Aug-T reference neurone A4 also had an offset trough in its phrenic spike-triggered average as detailed in Fig. 2 above. The I-Aug-T target cell, V3, first increased then decreased its activity during stimulation; it had no short time scale features in its phrenic spike-triggered average.

Cross-correlograms with significant features calculated from pairs composed of raphe and NTS neurones are listed in Table 7. Two examples are shown in Fig. 4. The firing rates of NTS reference neurones D5 and D4 increased during carotid chemoreceptor stimulation; the rates of the two target raphe neurones A6 and A9 did not change

significantly. A central peak is illustrated in the D5→A6 correlogram; neither neurone had a respiratory modulated firing rate. The cross-correlogram illustrates an increase in firing probability in the E-Decr-T raphe neurone A9 following spikes in D4.

Concurrent changes in firing probabilities of distributed brainstem neurones during 'spontaneous' switching between two modes of phrenic nerve discharge

During one recording of neurones in four brainstem regions, several diminutions in the amplitude of integrated phrenic activity occurred in the absence of any controlled or monitored perturbation (Fig. 5). Each of these alternating 'states' persisted for several minutes. Blood pressure was stable except when stimulation of carotid chemoreceptors elicited transient increases in phrenic activity. Periodic noxious stimuli (toe pinch) delivered to assess the level of anaesthesia produced no discernible changes in blood pressure or integrated phrenic activity.

The firing rate of raphe neurone A17 increased and decreased in each instance along with phrenic efferent activity. Another NRM raphe cell, A16, exhibited a concomitant converse change in firing rate. The firing rates of both neurones increased in response to carotid chemoreceptor stimuli as shown previously in Fig. 3. The firing rate of A17 increased briefly then declined, while the activity of A16 showed a delayed, but longer lasting increase. The A16→A17 cross-correlogram had a central

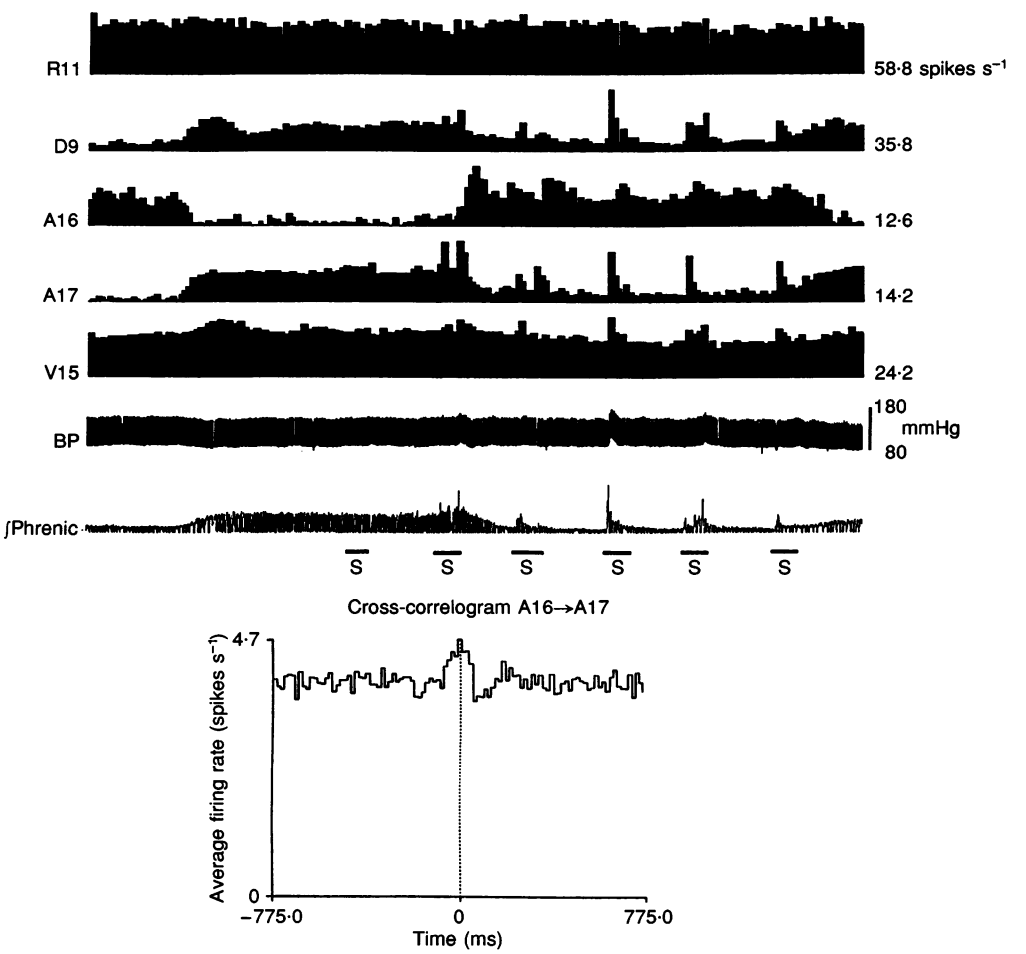

Figure 5. Long spontaneous changes in phrenic activity

Firing-rate histograms of 5 spike trains and integrated phrenic nerve activity over a period of 1000 s. Two raphe NRM neurones, A16 and A17, showed reciprocal changes with phrenic. The cross-correlogram shows a central peak (DI = 5·0; HW = 77·5 ms; 15506 trigger spikes; 22057 target spikes), an offset right trough (DI = 2·9; lag = 62·0 ms; HW = 46·5 ms) and an offset left trough (DI = 2·3; lag = 170·5 ms; HW = 31·0 ms). A16 and A17 alternated increases in activity in response to carotid chemoreceptor stimuli (see Fig. 3). R11, a rostral VRG, phasic, inspiratory neurone, showed no changes in activity during the spontaneous diminutions of phrenic activity, decreased activity during stimulation and had an offset peak in its spike-triggered average. D9 was an I-Aug-P NTS neurone, and V15, an I-Aug-T caudal VRG neurone; both showed changes corresponding to phrenic, increased activity with chemoreceptor stimulation and had central peaks in their spike-triggered averages.

peak and a pronounced offset trough with a positive lag; a secondary dip with a negative lag was also discernible.

R11, a phasic inspiratory rostral VRG neurone, showed no changes in activity during the spontaneous diminutions of phrenic activity; its firing probability decreased during chemoreceptor stimulation. In contrast, the phasic inspiratory DRG neurone D9, and tonic inspiratory caudal VRG neurone V15 both exhibited changes in rate that matched the direction of change in integrated phrenic amplitude during both spontaneous and chemoreceptor driven conditions. The phrenic spike-triggered average of neurone R11 had an offset peak with a positive lag. Cells D9 and V15 had central peaks in their phrenic spike-triggered averages.

DISCUSSION

The measurements described in this paper document changes in the firing rates of neurones in the region of nucleus raphe obscurus in response to carotid chemoreceptor stimulation. Concurrent changes in spike activity were monitored in neurones distributed among various other brainstem sites implicated in the control of breathing. Results of spike train cross-correlation analysis provided evidence for functional associations of chemoresponsive raphe neurones. In addition to links between raphe neurones, the data indicated effective connectivity of raphe neurones with neurones in the ventrolateral medulla and nucleus tractus solitarii. Spike-triggered averages of phrenic motor neurone activity also suggested paucisynaptic relationships.

The results support the view that chemoresponsive neurones in the raphe have effective connections appropriate for participation in the response of the respiratory system to carotid chemoreceptor stimulation. The data suggest several hypotheses about (a) the links that underlie synchrony of chemoresponsive raphe neurones, (b) the routes by which carotid chemoreceptors influence respiratory motor output, and (c) the transformation of information from those receptors. Simple interpretations of the classes of short time scale correlations found in this study and some of their implications are considered in the following paragraphs. The suggested connectivity schemes are intended to describe simple relationships sufficient to generate the detected correlations. Each inferred functional connection represents a subset of the anatomical connectivity that could underlie the results. It should be noted that we made no attempt to classify individual neurones as serotonergic based on the analysis of data in this study.

Correlations between raphe neurones and efferent phrenic nerve activity

Raphe neurones have been implicated in the control of respiratory motoneurone excitability in both the brainstem and spinal cord (Holtman *et al.* 1986; Lalley, 1986; Zahn, Ellenberger & Feldman, 1989; Pilowski, deCastro, Llewellyn-Smith, Lipski & Voss, 1990; Berger *et al.* 1992; Kubin, Tojima, Davies & Pack, 1992; Mitchell *et al.* 1992; Lindsay & Feldman, 1993). It is reasonable to suggest the hypothesis that the features in the spike-triggered averages reflect some combination of the effects of presynaptic synchronization and actions of raphe neurones at both bulbar and spinal levels. The spike trains of raphe neurones without spinal projections may be correlated with phrenic nerve discharge if they are linked with neurones that influence the motoneurones (Fig. 6*Aa*). Raphe neurones may be elements of synchronous assemblies (Lindsey, Hernandez, Morris & Shannon, 1992*a*; Lindsey, Hernandez, Morris, Shannon & Gerstein, 1992*b*) and coupled through cross-connections or shared inputs with premotor neurones of the ventrolateral medulla (Lindsey, Segers, Morris, Hernandez, Saporta & Shannon, 1994). An alternative arrangement (Fig. 6*Ab*) also includes direct or indirect action of bulbospinal raphe neurones on phrenic motoneurones. The offset peak and offset troughs were consistent with this possibility. The central troughs in the spike-triggered averages could reflect opposite actions on different pools that converge on the phrenic motoneurones (Fig. 6*Ac*) or actions of a synchronized pool of inhibitory or disfacilitatory neurones (Fig. 6*Ad*).

Functional links between raphe neurones and medullary neurones distributed in other sites

The NTS is reported to be the site where carotid chemoreceptor afferent axons make monosynaptic connections with second order neurones (Kirkwood, Nisimaru & Sears, 1979), and where most terminal arborizations of carotid sinus nerve afferents are located (Davies & Edwards, 1975; Donoghue, Felder, Jordan & Spyer, 1984; Grelot, Barillot & Bianchi, 1989; Finley & Katz, 1991). However, terminals have also been found in the ventrolateral medulla (Davies & Edwards, 1975; Grelot *et al.* 1989; Finley & Katz, 1991). Features of short time scale correlations between raphe neurones and chemoresponsive neurones in both the NTS and region of the caudal VRG (Fig. 4) suggest effective connections (Fig. 6*Ba* and *b*, respectively) that are consistent with the hypothesis that raphe neurones are influenced by carotid chemoreceptors through these putative parallel routes (Fig. 6*Bc*). Projections from the NTS and region of the VRG to the raphe have been reported (Connelly *et al.* 1989; Smith *et al.* 1989). Targets of projections from the ventrolateral medulla include serotonergic neurones in the medullary raphe nuclei (Zagon, 1993).

Primary features in cross-correlograms calculated with chemoresponsive raphe trigger neurones and caudal VRG target cells (Fig. 4) also suggest that chemoresponsive raphe neurones have excitatory or inhibitory actions on neurones in that lateral region (Fig. 6*C a* and *b*). The inferred connectivity is consistent with anatomical and other electrophysiological evidence for projections from neurones

in the mid-line raphe nuclei to the ventrolateral medulla (Connelly *et al.* 1989; Smith *et al.* 1989; Holtman, Marion & Speck, 1990; Lindsey *et al.* 1994). Note that the sign of the putative interaction was not always consistent with the direction of the changes in firing probability in response to chemoreceptor stimulation. For example, the responses and relationship shown in Fig. 6*Cb* are consistent with an inhibitory action of neurone A4 that contributed to the reduced firing probability of neurone V3 in response to chemoreceptor stimulation. However, the putative

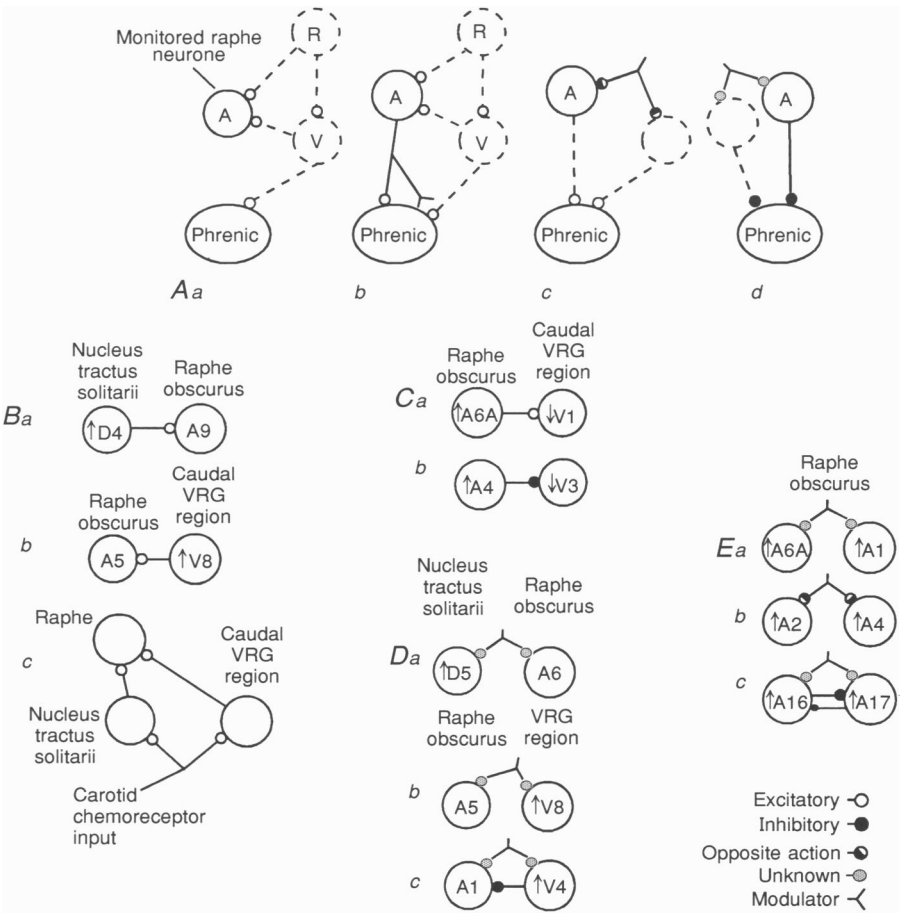

Figure 6. Connections inferred from cross-correlograms and spike-triggered averages

A a, copy of premotor (V) excitatory output, including influence of carotid chemoreceptors (R), is received by monitored raphe neurone (A). *A b*, monitored raphe neurone (A) has post- and/or presynaptic excitatory influence on phrenic motoneurones. *A c*, monitored raphe neurone with an excitatory influence on phrenic motoneurones has shared input of opposite sign with other premotor influence. *A d*, monitored raphe neurone has inhibitory influence on phrenic motoneurones and/or shared input of either sign with other premotor influence. *B*, *C* and *D* represent inferences from cross-correlograms in Fig. 4. *Ba*, excitatory effective connection from D4, an NRM neurone in NTS that responded to carotid chemoreceptor stimulation with increased activity, and A9, a raphe neurone with an expiratory modulated firing rate. *Bb*, an offset peak represents an excitatory connection from a chemoresponsive, respiratory modulated caudal VRG neurone (V8) to a raphe neurone (A5). *Bc*, excitatory input from carotid chemoreceptors is relayed to raphe through NTS and caudal VRG. *Ca*, raphe neurone A6A increases activity during carotid chemoreceptor stimulation and has an excitatory connection to caudal VRG neurone V1 that acts to limit the decrease of the latter during stimulation. *Cb*, A4, also in raphe, increases activity during stimulation and contributes to the decline in firing rate of V3 with an inhibitory connection. *Da*, NTS neurone D5 and raphe neurone A6 have a shared input. D5 increases activity during carotid chemoreceptor stimulation; A6 does not. Neither had a respiratory modulated firing rate. *Db*, an alternative explanation for an offset peak (V8→A5) is a shared input through paths that reach caudal VRG neurones with a shorter delay than that to raphe neurones. *Dc*, central peak and offset trough may represent a shared input of A1 and V4 with an inhibitory connection from the latter to the former. *Ea*, two raphe neurones A6A and A1 increase activity during stimulation and have a shared input (Fig. 4). *Eb*, A2 and A4 have a shared input of opposite sign. *Ec*, A16 and A17 (Figs 3 and 5) have a shared input and mutual inhibitory connections.

excitatory action of neurone A6A on cell V1 (Fig. 6*Ca*) implies that the connection does not contribute to the decline in activity in neurone V1. This apparent discrepancy is not cause to reject the inferred sign of the connection; the arrangement could represent a relationship that tends to limit the decline in firing probability generated by another unobserved parallel path that carries chemoreceptor information.

Correlations between raphe neurones and cells in the other two regions also suggested the influence of unobserved shared inputs. Some parsimonious interpretations are shown in Fig. 6*D*. The central peak in the D5→A6 cross-correlogram in Fig. 4 suggests that chemoresponsive neurones in the nucleus tractus solitarii and neurones in nucleus raphe obscurus are co-ordinated by shared inputs (Fig. 6*Da*); this interpretation is consistent with the arrangement illustrated in Fig. 6*Bc*. For the sake of completeness, Fig. 6*Db* shows an alternative interpretation of data such as that illustrated by offset features in cross-correlograms in Fig. 4. The delayed effects of a shared input at one of two neurones relative to the other can produce an offset feature in a cross-correlogram. Correlogram features suggestive of concurrent shared inputs and inhibition of raphe neurones by chemoresponsive ventrolateral medullary neurones were also detected as exemplified in the V4→A1 cross-correlogram in Fig. 4. A scheme illustrating this possibility is shown in Fig. 6*Dc*. Inhibition of A1 by V4 could contribute to the respiratory modulation of the former neurone. An alternative interpretation of the unilateral offset trough is a greater tendency of A1 than V4 to become refractory following spikes contributed to by their shared input.

Inferred interactions between raphe neurones

The detection of the major classes of primary features in cross-correlograms (central peaks and troughs and offset peaks and troughs) for pairs of raphe neurones confirm and extend previously reported results (Lindsey *et al.* 1992*a*). In the present work, seventeen pairs of raphe neurones exhibited primary and secondary features in their cross-correlograms suggestive of shared inputs as well as reciprocal excitatory or inhibitory connections (Fig. 6*E*).

In twenty-one pairs of simultaneously monitored raphe neurones, the two neurones exhibited sequential increases in firing rate in response to carotid chemoreceptor stimulation. Data from one of these pairs, neurones A16 and A17, were illustrated in Figs 3 and 5. Neither neurone had a respiratory-modulated firing rate. The firing rate of one neurone increased transiently, whereas the other neurone showed a longer-lasting increase that began only as the rate of the first declined. The transient nature of the faster response could reflect an inhibitory action of neurones with the delayed response. Simple interpretations of the primary features in the cross-correlogram for the two raphe neurones are consistent with these possibilities (Fig. 6*Ec*). The central peak was evidence of a shared input. The primary offset trough with a positive lag in the cross-correlogram may represent a potent inhibition with a lag of about 45 ms that could suppress the faster response exhibited by neurone A17. The 'weak' (DI = 2·3) dip with a long negative lag time may reflect an asymmetrical reciprocal inhibitory effect. Similar correlograms for pairs of raphe neurones have been described previously (Fig. 13 in Lindsey *et al.* 1992*a*). The sequential responses to carotid chemoreceptor stimulation were also consistent with the

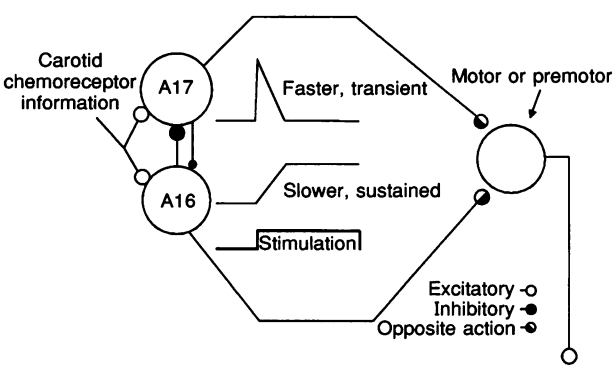

Figure 7. Responses to changes in respiratory drive, including carotid chemoreceptor stimulation, of phrenic nerve and lateral brainstem and raphe neurones in an experiment with several spontaneous changes in phrenic activity

A17 increases along with phrenic activity whilst A16 decreases, possibly in part due to increased inhibition from A17. An unknown factor changes the balance of inhibition. A17 decreases activity along with phrenic as A16 increases. During carotid chemoreceptor stimulation, both neurones are excited although the response of A17 might delay that of A16. However, as A16 increases activity it inhibits A17. An excitatory effective connection to phrenic motoneurones from A17 and an inhibitory one from A16 would contribute to the observed changes in phrenic activity. Alternatively, an inhibitory effective connection to phrenic motoneurones from A17 and an excitatory one from A16 would act to limit changes in phrenic nerve activity during different levels of drive.

possibility that both neurones were excited by chemoreceptor stimulation through parallel channels with different conduction velocities, routes, or synaptic mechanisms.

The time course of the responses and inferred connections of the raphe neurones support the hypothesis that mid-line respiratory-related neuronal assemblies use recurrent inhibitory connections in an internal equilibrium seeking system that acts to stabilize and regulate the gain of respiratory motor output (Lindsey *et al.* 1992*b*). The switching between two modes of firing probability that was co-ordinated with respiratory motoneurone activity is also consistent with this idea.

Figure 7 is a composite of interpretations of data shown in Figs 3 and 5. The opposite changes in firing rate that matched the long, spontaneous reciprocal changes in phrenic motoneurone discharge suggest that NRM raphe neurones A16 and A17 shared unpatterned drive in common with respiratory (pre) motoneurones including input from carotid chemoreceptors. Another possibility is that, as considered above, the raphe neurones modulate the motoneurones at spinal or brainstem levels. These possibilities are not mutually exclusive.

The 'spontaneous' and experimentally evoked changes in firing rates of neurones in the ventrolateral medulla that were recorded simultaneously with raphe neurones A16 and A17 suggest that the changes in phrenic activity reflected the consequences of descending influences. The rostral VRG neurone R11 (Fig. 5) had a cycle-triggered histogram similar to the previously described, putative I-Driver neurones involved in timing of the respiratory rhythm (Segers *et al.* 1987). These neurones begin activity in late expiratory or early inspiratory phase and show a slight decline in activity until the end of inspiration, then a relatively abrupt termination. The offset peak in its spike-triggered average suggests that R11 has an excitatory effect upon phrenic motoneurones and supports its characterization as an I-Driver. R11 continued unchanged during motor output amplitude oscillations yet decreased its firing rate, as inspiratory duration decreased, during carotid chemoreceptor stimulation.

Caudal VRG inspiratory neurone V15 and DRG inspiratory neurone D9 increased and decreased firing rates when phrenic activity spontaneously increased and decreased. They also increased activity during the phrenic response to carotid chemoreceptor stimulation. Central peaks in their spike-triggered averages suggest that they share input with phrenic motoneurones. Because some premotor drive of phrenic motoneurones originates in the caudal VRG and DRG (Cohen, Piercey, Gootman & Wolotsky, 1974; Davies, Kirkwood & Sears, 1985), the central peaks may indicate that D9 and V15 are members of populations that provide this premotor drive. It is reasonable to speculate that the changes in phrenic nerve discharge were caused, at least in part, by changes in the activity of medullary neurone populations. The spontaneous changes in firing rate of neurones R11, V15, and D9 and their responses to chemoreceptor stimulation were consistent with the model for parallel control of inspiratory drive and phase duration proposed elsewhere (Morris *et al.* 1996).

Other implications

Five raphe neurones changed firing rate in the same direction during both carotid chemo- and baroreceptor stimulation. The change during chemoreceptor stimuli may have been due, entirely or in part, to stimulation of baroreceptors by the reflex increase in blood pressure (see Fig. 1). These changes could also represent a convergence of input. The latter interpretation is consistent with the seven raphe neurones that changed firing rate during both kinds of stimuli but in opposite directions. Preliminary analysis of the convergence of carotid chemoreceptor and baroreceptor stimulation has been reported (Morris, Arata, Shannon & Lindsey, 1994).

This investigation of the responses of raphe neurones to carotid chemoreceptor stimulation was motivated by their postulated participation in the long-term facilitation of respiration (Millhorn *et al.* 1980; Millhorn, 1986). The analysis of their immediate responses and effective connectivity reported here represents a step in testing that hypothesis. There is no long-term facilitation seen with CO_2 stimulation of central chemoreceptors (Millhorn et al. 1980). The results of this study suggest that CO_2 stimulation of peripheral chemoreceptors produces a long-term facilitation of phrenic nerve activity qualitatively similar to electrical or hypoxic stimulation (compare Fig. 1*A* here with Millhorn *et al.* 1980, Fig. 1). The protocol of these experiments precluded an investigation into the response of raphe neurones, or the lateral neurones that communicate with them, to central chemoreceptor stimulation. This study provided evidence for the relay of excitatory input from the carotid chemoreceptors to the raphe obscurus via neurones in the NTS. It also provided evidence for the relay of this excitatory input via respiratory modulated VRG neurones. It remains to be shown if the input from carotid chemoreceptors to raphe neurones through one or both of these paths is functionally antecedent to convergence with central chemoreceptor input.

Aertsen, A. M. H. J. & Gerstein, G. L. (1985). Evaluation of neuronal connectivity: sensitivity of cross-correlation. *Brain Research* **340**, 341–354.

Berger, A. J., Bayliss, D. A. & Viana, F. (1992). Modulation of neonatal rat hypoglossal motoneuron excitability by serotonin. *Neuroscience Letters* **143**, 164–168.

BRODIN, E., LINDEROTH, B., GOINY, M., YAMAMOTO, Y., GAZELIUS, B., MILLHORN, D. E., HOKFELT, T. & UNGERSTEDT, U. (1990). *In vivo* release of serotonin in cat dorsal vagal complex and cervical ventral horn induced by electrical stimulation of the medullary raphe nuclei. *Brain Research* **535**, 227–236

COHEN, M. I., PIERCEY, M. F., GOOTMAN, P. M. & WOLOTSKY, P. (1974). Synaptic connections between medullary inspiratory neurones and phrenic motoneurons as revealed by cross-correlation. *Brain Research* **81**, 319–324.

CONNELLY, C. A., ELLENBERGER, H. H. & FELDMAN, J. L. (1989). Are there serotonergic projections from the raphe and retrotrapeziod nuclei to the ventral respiratory group in the rat? *Neuroscience Letters* **105**, 34–40.

DAVEY, N. J., ELLAWAY, P. H. & STEIN, R. B. (1986). Statistical limits for detecting change in the cumulative sum derivative of the peristimulus time histogram. *Journal of Neuroscience Methods* **17**, 153–166.

DAVIES, J. G. McF., KIRKWOOD, P. A. & SEARS, T. A. (1985). The distribution of monosynaptic connexions from inspiratory bulbospinal neurons to inspiratory motoneurones in the cat. *Journal of Physiology* **368**, 63–87.

DAVIES, R. O. & EDWARDS, M. W. JR (1975). Medullary relay neurons in the carotid body chemoreceptor pathway of cats. *Respiration Physiology* **24**, 69–79.

DONOGHUE, S., FELDER, R. B., JORDAN, D. & SPYER, K. M. (1984). The central projections of carotid baroreceptors and chemoreceptors in the cat: a neurophysiological study. *Journal of Physiology* **347**, 397–409.

FINLEY, J. C. W. & KATZ, D. M. (1991). The central organization of carotid body afferent projections to the brainstem of the rat. *Brain Research* **572**, 108–116.

GRELOT, L., BARILLOT, J. C. & BIANCHI, A. L. (1989). Central distributions of the efferent and afferent components of the pharyngeal branches of the vagus and glossopharyngeal nerves: an HRP study in the cat. *Experimental Brain Research* **78**, 327–335.

HOLTMAN, J. R. JR, DICK, T. E. & BERGER, A. J. (1986). Involvement of serotonin in the excitation of phrenic motoneurons evoked by stimulation of the raphe obscurus. *Journal of Neuroscience* **6**, 1185–1193.

HOLTMAN, J. R. JR, MARION, L. J. & SPECK, D. F. (1990). Origin of serotonin-containing projections to the ventral respiratory group in the rat. *Neuroscience* **37**, 541–552.

JACOBS, B. L. & AZMITE, E. C. (1992). Structure and function of the brain-serotonin system. *Physiological Reviews* **72**, 165–229.

KIRKWOOD, P. A., NISIMARU, N. & SEARS, T. A. (1979). Monosynaptic excitation of bulbospinal respiratory neurones by chemoreceptor afferents in the carotid sinus nerve. *Journal of Physiology* **293**, 35–36*P*.

KUBIN, L., TOJIMA, H., DAVIES, R. O. & PACK, A. I. (1992). Serotonergic excitatory drive to hypoglossal motoneurons in the decerebrate cat. *Neuroscience Letters* **139**, 243–248.

LALLEY, P. M. (1986). Serotoninergic and non-serotoninergic responses of phrenic motoneurones to raphe stimulation in the cat. *Journal of Physiology* **380**, 373–385.

LINDSAY, A. D. & FELDMAN, J. L. (1993). Modulation of respiratory activity of neonatal rat phrenic motoneurons by serotonin. *Journal of Physiology* **461**, 213–233.

LINDSEY, B. G., HERNANDEZ, Y. M., MORRIS, K. F. & SHANNON, R. (1992*a*). Functional connectivity between brain stem midline neurons with respiratory-modulated firing rates. *Journal of Neurophysiology* **67**, 890–904.

LINDSEY, B. G., HERNANDEZ, Y. M., MORRIS, K. F., SHANNON, R. & GERSTEIN, G. L. (1992*b*). Dynamic reconfiguration of brain stem neural assemblies: respiratory phase-dependent synchrony *versus* modulation of firing rates. *Journal of Neurophysiology* **67**, 923–930.

LINDSEY, B. G., SEGERS, L. S., MORRIS, K. F., HERNANDEZ, Y. M., SAPORTA, S. & SHANNON, R. (1994). Distributed actions and dynamic associations in respiratory-related neuronal assemblies of the ventrolateral medulla and brain stem midline: Evidence from spike train analysis. *Journal of Neurophysiology* **72**, 1830–1851.

MILLHORN, D. E., ELDRIDGE, F. L. & WALDROP, T. G. (1980). Prolonged stimulation of respiration by endogenous central serotonin. *Respiration Physiology* **42**, 171–188.

MILLHORN, D. E. (1986). Stimulation of raphe (obscurus) nucleus causes long-term potentiation of phrenic nerve activity in cat. *Journal of Physiology* **381**, 169–179.

MITCHELL, G. S., SLOAN, H. E., JIANG, C., MILETIC, V., HAYASHI, F. & LIPSKI, J. (1992). 5-Hydroxytryptophan (5-HTP) augments spontaneous and evoked phrenic motoneuron discharge in spinalized rats. *Neuroscience Letters* **141**, 75–78.

MIURA, M. & REIS, D. J. (1969). Termination and secondary projections of the carotid sinus nerve in the cat brain stem. *American Journal of Physiology* **217**, 142–153.

MONTEAU, R., MORIN, D., HENNEQUIN, S. & HILAIRE, G. (1990). Differential effects of serotonin on respiratory activity of hypoglossal and cervical motoneurons: an *in vitro* study on the newborn rat. *Neuroscience Letters* **111**, 127–132.

MORRIS, K. F., ARATA, A., SHANNON, R. & LINDSEY, B. G. (1993). Concurrent, distributed alterations in brain stem neural assemblies during induction of long-term enhancement of respiratory activity *in vivo* by carotid chemoreceptor stimulation. *Society for Neuroscience Abstracts* **19**, 574.4.

MORRIS, K. F., ARATA, A., SHANNON, R. & LINDSEY, B. G. (1994). Convergence of carotid chemoreceptor and baroreceptor inputs to distributed brain stem respiratory neural networks. *Society for Neuroscience Abstracts* **20**, 133.5.

MORRIS, K. F., ARATA, A., SHANNON, R. & LINDSEY, B. G. (1996). Inspiratory drive and phase duration during carotid chemoreceptor stimulation: medullary neurone correlations. *Journal of Physiology* (in the Press).

MORRISON, S. F. & GEBBER, G. L. (1984). Raphe neurons with sympathetic-related activity: baroreceptor responses and spinal connections. *American Journal of Physiology* **246**, R338–348.

OREM, J. & DICK, T. (1983). Consistency and signal strength of respiratory neuronal activity. *Journal of Neurophysiology* **50**, 1098–1107.

PALKOVITS, M., BROWNSTERN, M. & SAAVEDRA, J. (1974). Serotonin content of the brain stem nuclei in the cat. *Brain Research* **80**, 237–249.

PILOWSKI, P. M., DE CASTRO, D., LLEWELLYN-SMITH, I., LIPSKI, J. & VOSS, M. D. (1990). Serotonin immunoreactive boutons make synapses with feline phrenic motoneurons. *Journal of Neuroscience* **10**, 1091–1098.

SEGERS, L. S., SHANNON, R., SAPORTA, S. & LINDSEY, B. G. (1987). Functional associations among simultaneously monitored lateral medullary respiratory neurons in the cat. I: Evidence for excitatory and inhibitory actions of inspiratory neurons. *Journal of Neurophysiology* **57**, 1078–1100.

SMITH, J. C., MORRISON, D. E., ELLENBERGER, H. H., OTTO, M. R. & FELDMAN, J. L. (1989). Brain stem projections to the major respiratory neuron populations in the medulla of the cat. *Journal of Comparative Neurology* **281**, 69–96.

White, S. R. & Fung, S. J. (1989). Serotonin depolarizes cat spinal motoneurons in situ and decreases motoneuron after hyperpolarizing potentials. *Brain Research* **502**, 205–213.

Zagon, A. (1993). Innervation of serotonergic medullary raphe neurons from cells of the rostral ventrolateral medulla in rats. *Neuroscience* **55**, 849–867.

Zahn, W. Z., Ellenberger, H. H. & Feldman, J. L. (1989). Monoaminergic and GABAergic terminations in phrenic nucleus of rat identified by immunohistochemical labelling. *Neuroscience* **31**, 105–113.

Acknowledgements

This work was supported by NIH grants NS19814 and BRSG SO7 RR05749. The authors thank J. Gilliland, C. Orsini, D. Baekey and K. D. Morris for excellent technical assistance.

Author's present address

Dr Arata: Second Department of Physiology, Showa University School of Medicine, Tokyo, Japan.

Received 4 November 1994; *accepted 19 July 1995.*